

Supplementary: Unsupervised Deep Learning for FOD-Based Susceptibility Distortion Correction in Diffusion MRI

Yuchuan Qiao, Yonggang Shi

I. MORE EXPERIMENTAL RESULTS

In this supplementary, we provide more qualitative comparisons of distortion correction from different methods.

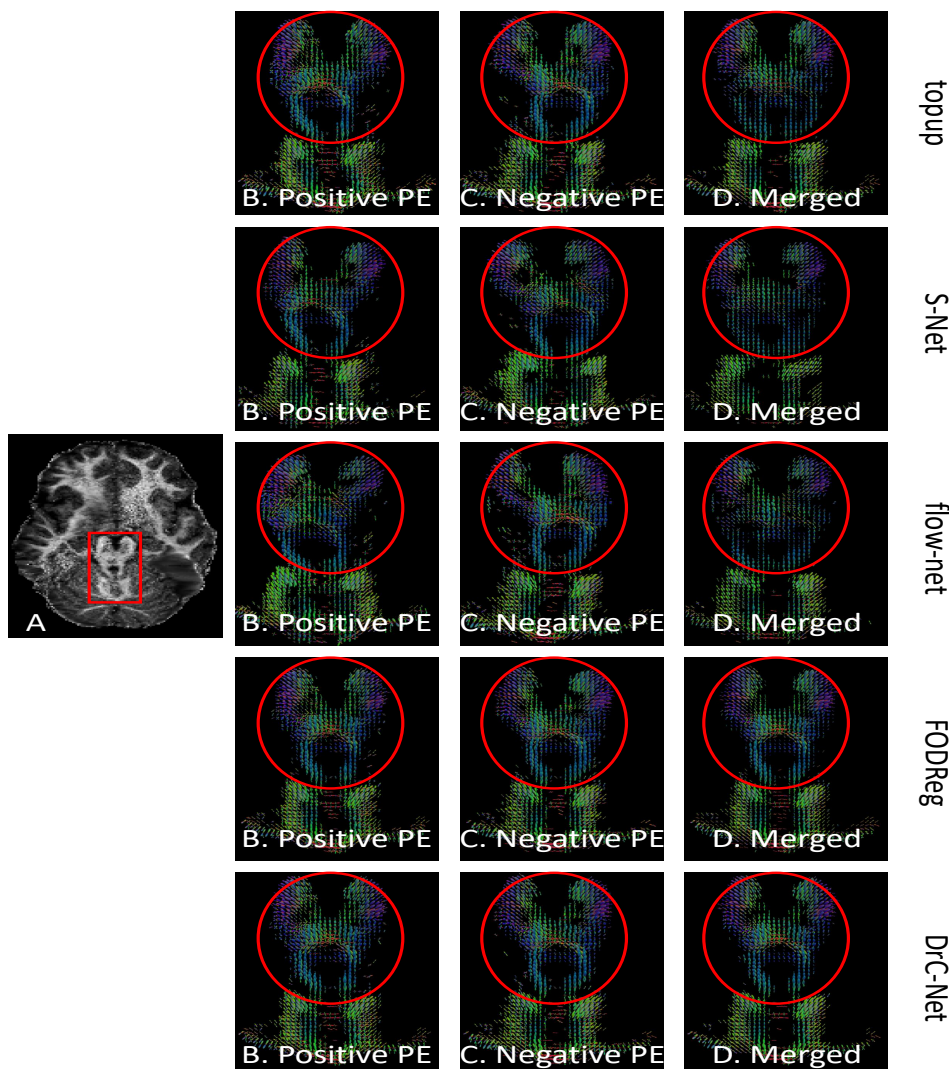


Fig. 1. Distortion correction effects shown in FOD images in the brainstem region for subject 118730 from HCP. (A) is the axial view of the first coefficient image of the FOD image. The five rows are for $topup$, S-Net, flow-net, FODReg and the proposed method, respectively. (B) (E), (H), (K) and (N) are FODs from the positive PE, while (C), (F), (I), (L) and (O) are FODs from the negative PE. The last column shows the FODs from the merged data after correction with different methods.

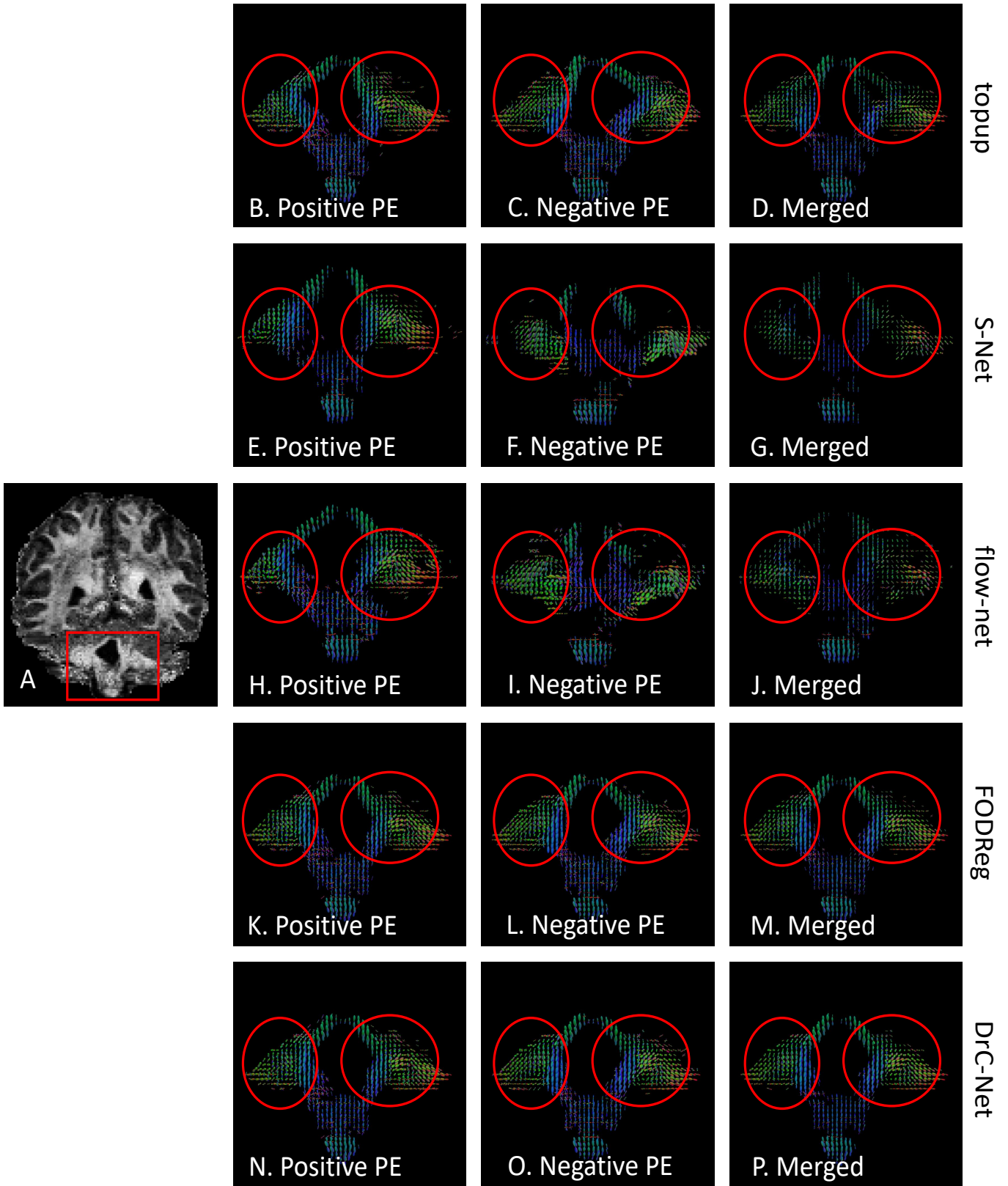


Fig. 2. Distortion correction effects shown in FOD images in the brainstem region for subject 107725 from HCP. (A) is the coronal view of the first coefficient image of the FOD image. The five rows are for topup , S-Net, flow-net, FODReg and the proposed method, respectively. (B) (E), (H), (K) and (N) are FODs from the positive PE, while (C), (F), (I), (L) and (O) are FODs from the negative PE. The last column shows the FODs from the merged data after correction with different methods.

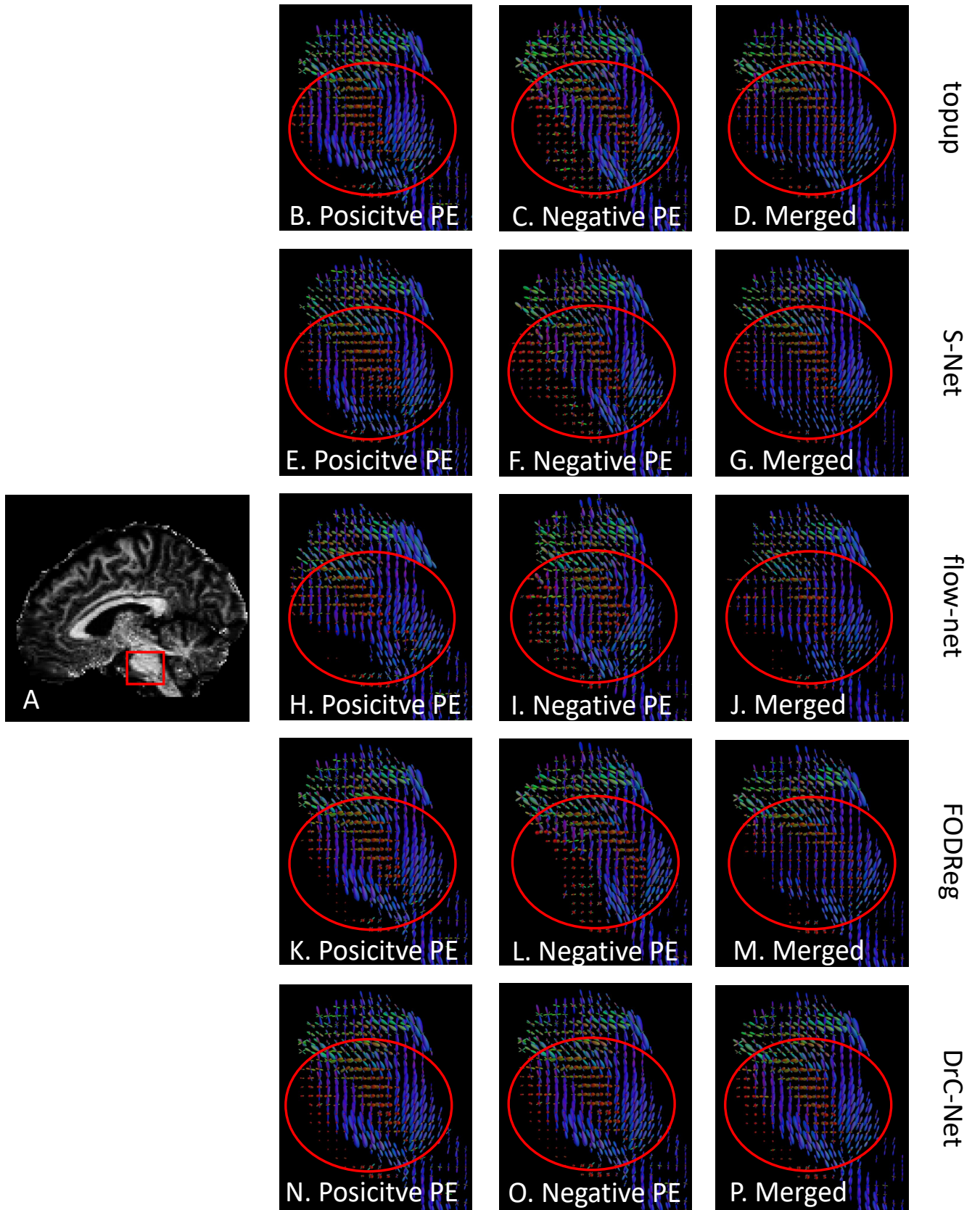


Fig. 3. Distortion correction effects shown in FOD images in the brainstem region for subject 3007 from HCLV. (A) is the sagittal view of the first coefficient image of the FOD image. The five rows are for topup , S-Net, flow-net, FODReg and the proposed method, respectively. (B) (E), (H), (K) and (N) are FODs from the positive PE, while (C), (F), (I), (L) and (O) are FODs from the negative PE. The last column shows the FODs from the merged data after correction with different methods.